

Parallel Flow-Based Hypergraph Partitioning

Lars Gottesbüren ✉

Karlsruhe Institute of Technology, Karlsruhe, Germany

Tobias Heuer ✉

Karlsruhe Institute of Technology, Karlsruhe, Germany

Peter Sanders ✉

Karlsruhe Institute of Technology, Karlsruhe, Germany

Abstract

We present a shared-memory parallelization of *flow-based refinement*, which is considered the most powerful iterative improvement technique for hypergraph partitioning at the moment. Flow-based refinement works on bipartitions, so current sequential partitioners schedule it on different block pairs to improve k -way partitions. We investigate two different sources of parallelism: a parallel scheduling scheme and a parallel maximum flow algorithm based on the well-known push-relabel algorithm. In addition to thoroughly engineered implementations, we propose several optimizations that substantially accelerate the algorithm in practice, enabling the use on extremely large hypergraphs (up to 1 billion pins). We integrate our approach in the state-of-the-art parallel multilevel framework Mt-KaHyPar and conduct extensive experiments on a benchmark set of more than 500 real-world hypergraphs, to show that the partition quality of our code is on par with the highest quality sequential code (KaHyPar), while being an order of magnitude faster with 10 threads.

2012 ACM Subject Classification Mathematics of computing → Hypergraphs; Mathematics of computing → Graph algorithms

Keywords and phrases multilevel hypergraph partitioning, shared-memory algorithms, maximum flow

Supplementary Material

Source code (multilevel framework): <https://github.com/kahypar/mt-kahypar>

Source code (flow-based refinement): <https://github.com/larsgottesbueren/WHFC/tree/parallel>

Benchmark Set & Experimental Results: <https://algo2.iti.kit.edu/heuer/sea22/>

Funding This work was partially supported by DFG grants WA654/19-2 and SA933/11-1. The authors acknowledge support by the state of Baden-Württemberg through bwHPC.

1 Introduction

Balanced hypergraph partitioning is a classical NP-hard optimization problem with numerous applications. Hypergraphs are a generalization of graphs, where each hyperedge can connect an arbitrary number of vertices. The problem is to partition the vertices of a hypergraph $H = (V, E, \omega)$ into k disjoint blocks V_1, \dots, V_k of roughly equal size ($\forall V_i : |V_i| \leq (1 + \varepsilon) \frac{|V|}{k}$), such that an objective function defined on the hyperedges is minimized. In this work, we consider the connectivity metric $\sum_{e \in E} (\lambda(e) - 1) \omega(e)$ where $\lambda(e) := |\{V_i \mid e \cap V_i \neq \emptyset\}|$ denotes the number of different blocks connected by hyperedge $e \in E$ and $\omega(e)$ denotes its weight. Often balanced partitioning is used as an acceleration technique for other applications, such as quantum circuit simulation [31], sharding distributed databases [15, 36], load balancing (for scientific computing) [13], route planning [17, 32], or boosting cache utilization in a search engine backend [7].

There is a substantial amount of literature on graph and hypergraph partitioning, which is why we refer to survey articles [4, 9, 50, 55] for a summary. Due to being NP-hard [46] and hard to approximate within constant factors [12], most of the work focuses on heuristic algorithms, with the multilevel paradigm emerging as the most successful and widely used approach in

modern partitioners [2, 13, 19, 30, 38, 44, 54, 55]. Most partitioners use variations of well-known local vertex moving heuristics such as Kernighan-Lin [41] or Fiduccia-Mattheyses [22]. However, these techniques are known to easily get stuck in local minima [42].

In this situation, maximum flows are an excellent tool as they correspond to (unbalanced) minimum cuts, thus offering a more global view than local routines. While being a fundamental algorithmic tool, maximum flows were long overlooked for partitioning heuristics, due to their complexity [60], but have since enjoyed wide-spread adoption [5, 17, 32, 43, 54, 60] in many different algorithmic contexts, even outside the multilevel framework.

Contribution. In this paper, we parallelize *flow-based refinement*, a powerful technique that is the last missing component in a series of works [28, 30] on parallelizing the state-of-the-art multilevel hypergraph partitioning framework KaHyPar [55]. Flow-based refinement operates on bipartitions, or on two blocks at a time if used for $k > 2$. Scheduling independent block pairs gives some trivial parallelism. One contribution we make is to improve the parallelism in the scheduler by relaxing certain constraints of the original approach and showing how to deal with race conditions caused by the relaxation. For small k this is still insufficiently parallel, which is why we also parallelize the refinement on two blocks. We adapt an existing parallel flow algorithm to handle the incremental flow problems of the FlowCutter refinement algorithm [26, 27, 32]. Additionally, we engineer an efficient implementation, proposing several optimizations that reduce running time in practice, and fix a so far not documented bug in the parallel flow algorithm itself, not the implementation. The result is a partitioning framework that achieves the same solution quality as the highest quality sequential framework, but in a fast parallel code. Using 10 threads, our code is an order of magnitude faster than sequential KaHyPar with flow-based refinement.

Outline. The paper is organized as follows. In Section 2 we introduce notation, terminology, and some algorithmic preliminaries. Section 3 briefly deals with related work. More details on additional related work are given in the main sections 5 - 8, closer to where particular parts are needed. In Section 4, we give an overview of the different components in the framework and how they interact. We complement the algorithmic discussion with extensive experiments in Section 10, before concluding in Section 11.

2 Preliminaries

Hypergraphs. A *weighted hypergraph* $H = (V, E, c, \omega)$ is defined as a set of vertices V and a set of hyperedges/nets E with vertex weights $c : V \rightarrow \mathbb{R}_{>0}$ and net weights $\omega : E \rightarrow \mathbb{R}_{>0}$, where each net e is a subset of the vertex set V . The vertices of a net are called its *pins*. We extend c and ω to sets in the natural way, i.e., $c(U) := \sum_{v \in U} c(v)$ and $\omega(F) := \sum_{e \in F} \omega(e)$. A vertex v is *incident* to a net e if $v \in e$. $I(v)$ denotes the set of all incident nets of v . The *degree* of a vertex v is $d(v) := |I(v)|$. The *size* $|e|$ of a net e is the number of its pins. We call two nets e_i and e_j *identical* if $e_i = e_j$. Given a subset $V' \subset V$, the *subhypergraph* $H_{V'}$ is defined as $H_{V'} := (V', \{e \cap V' \mid e \in E : e \cap V' \neq \emptyset\})$.

Balanced Hypergraph Partitioning. A *k-way partition* of a hypergraph H is a function $\Pi : V \rightarrow \{1, \dots, k\}$. The blocks $V_i := \Pi^{-1}(i)$ of Π are the inverse images. We call Π *ε -balanced* if each block V_i satisfies the *balance constraint*: $c(V_i) \leq L_{\max} := (1 + \varepsilon) \lceil \frac{c(V)}{k} \rceil$ for some parameter $\varepsilon \in (0, 1)$. For each net e , $\Lambda(e) := \{V_i \mid V_i \cap e \neq \emptyset\}$ denotes the *connectivity set* of e . The *connectivity* $\lambda(e)$ of a net e is $\lambda(e) := |\Lambda(e)|$. A net is called a *cut net* if $\lambda(e) > 1$. A node u that is incident to at least one cut net is called *boundary node*. The number of pins of a net e in block V_i is denoted by $\Phi(e, V_i) := |e \cap V_i|$. The *quotient graph* $\mathcal{Q} := (\Pi, E_{\Pi} := \{(V_i, V_j) \mid \exists e \in E : \{V_i, V_j\} \subseteq \Lambda(e)\})$ contains an edge between each pair of

adjacent blocks of a k -way partition Π . Given parameters ε and k , and a hypergraph H , the *balanced hypergraph partitioning problem* is to find an ε -balanced k -way partition Π that minimizes an objective function defined on the hyperedges. In this work, we minimize the *connectivity metric* $(\lambda - 1)(\Pi) := \sum_{e \in E} (\lambda(e) - 1) \omega(e)$.

Flows. A flow network $\mathcal{N} = (\mathcal{V}, \mathcal{E}, c)$ is a directed graph with a dedicated source $s \in \mathcal{V}$ and sink $t \in \mathcal{V}$ in which each edge $e \in \mathcal{E}$ has capacity $c(e) \geq 0$. An (s, t) -flow is a function $f : \mathcal{V} \times \mathcal{V} \rightarrow \mathbb{R}$ that satisfies the *capacity constraint* $\forall u, v \in \mathcal{V} : f(u, v) \leq c(u, v)$, the *skew symmetry constraint* $\forall u, v \in \mathcal{V} : f(u, v) = -f(v, u)$ and the *flow conservation constraint* $\forall u \in \mathcal{V} \setminus \{s, t\} : \sum_{v \in \mathcal{V}} f(u, v) = 0$. The value of a flow $|f| := \sum_{v \in \mathcal{V}} f(s, v) = \sum_{v \in \mathcal{V}} f(v, t)$ is defined as the total amount of flow transferred from s to t . An (s, t) -flow f is a maximum (s, t) -flow if there exists no other (s, t) -flow f' with $|f| < |f'|$. The *residual capacity* is defined as $r_f(e) = c(e) - f(e)$. An edge e is *saturated* if $r_f(e) = 0$. $\mathcal{N}_f = (\mathcal{V}, \mathcal{E}_f, r_f)$ with $\mathcal{E}_f := \{(u, v) \in \mathcal{V} \times \mathcal{V} \mid r_f(u, v) > 0\}$ is the *residual network*. The max-flow min-cut theorem states that the value $|f|$ of a maximum (s, t) -flow equals the weight of a minimum cut that separates s and t [23]. This is also called a *minimum (s, t) -cut*. The source-side cut can be computed by BFS from the source via residual edges, the sink-side cut via reverse BFS from the sink.

Push-Relabel Algorithm. The *push-relabel* [24] maximum flow algorithm stores a distance label $d(u)$ and an excess value $\text{exc}(u) := \sum_{v \in \mathcal{V}} f(v, u)$ for each node. It maintains a *preflow* [40] which is a flow where the conservation constraint is replaced by $\text{exc}(u) \geq 0$. A node $u \in \mathcal{V}$ is *active* if $\text{exc}(u) > 0$. An edge $(u, v) \in \mathcal{E}$ is *admissible* if $r_f(u, v) > 0$ and $d(u) = d(v) + 1$. A *push* (u, v) operation sends $\delta = \min(\text{exc}(u), r_f(u, v))$ flow units over (u, v) . It is applicable if u is active and (u, v) is admissible. A *relabel* (u) operation updates the distance label of u to $\min(\{d(v) + 1 \mid r_f(u, v) > 0\})$, which is applicable if u is active has no admissible edges. The distance labels are initialized to $\forall u \in \mathcal{V} - s : d(u) = 0$ and $d(s) = |\mathcal{V}|$ and all source edges are saturated. Efficient variants use the *discharge* routine, which repeatedly scans the edges of an active node until its excess is zero. All admissible edges are pushed and at the end of a scan, the node is relabeled. Discharging active nodes in FIFO order results in an $\mathcal{O}(|\mathcal{V}|^3)$ time algorithm. The *global relabeling* heuristic [14] frequently assigns exact distance labels by performing a reverse BFS from the sink, to reduce relabel work in practice. Preflows already induce minimum sink-side cuts, so if only cuts are required, the algorithm can already stop once no active nodes with distance label $< n$ exist.

Flows on Hypergraphs. The *Lawler expansion* [45] of a hypergraph $H = (V, E, c, \omega)$ is a graph consisting of V and two nodes $e_{\text{in}}, e_{\text{out}}$ for each $e \in E$, with directed edges $\forall u \in V, e \in E : (u, e_{\text{in}}), (e_{\text{out}}, u)$ with infinite capacity and bridging edges $\forall e \in E : (e_{\text{in}}, e_{\text{out}})$ with capacity $\omega(e)$. A minimum (s, t) -cut in the Lawler expansion directly corresponds to one in the hypergraph.

3 Related Work

There is a vast amount of literature on hypergraph partitioning, including extensive surveys [4, 9, 50, 55]. The most relevant sequential algorithms are PaToH [13], hMetis [38, 39], and KaHyPar [1, 26, 56]. Notable parallel algorithms are Parkway [58] and Zoltan [19] for distributed memory, as well as BiPart [47] and Mt-KaHyPar [28, 30] for shared memory.

All of these follow the multilevel paradigm that proceeds in three phases: First, the hypergraph is *coarsened* to obtain a hierarchy of successively smaller and structurally similar hypergraphs by *contracting* pairs or clusters of vertices. Once the coarsest hypergraph is small enough, an *initial partition* into k blocks is computed. Subsequently, the contractions

are reverted level-by-level, and, on each level, *local search* heuristics are used to improve the partition from the previous level (*refinement phase*).

Sanders and Schulz [54] propose an algorithm to improve the edge cut of bipartitions with flow-based refinement. Their general idea is to grow a size-constrained region around the cut edges of a bipartition. Afterwards, they compute a minimum (s, t) -cut in the subgraph induced by the region and apply it to the original graph, if it satisfies the balance constraint. They extended their algorithm to k -way partitions by scheduling it on pairs of adjacent blocks. Heuer et al. [33] integrated this approach into their hypergraph partitioner KaHyPar. The framework was then further improved by Gottesbüren et al. [26] by replacing the bipartitioning routine with the FlowCutter algorithm [27, 32]. Flow-based refinement substantially improved the solution quality (connectivity metric) of the partitions produced by KaHyPar, making it the method of choice for high-quality hypergraph partitioning [55]. We will explain the flow-based refinement routine of KaHyPar in more detail in the main part of our work. Notable other flow-based refinement algorithms are Improve [5] and MQI [43], which improve the expansion or conductance metric of bipartitions.

4 Framework Overview

Algorithm 1 Parallel Flow-Based Refinement

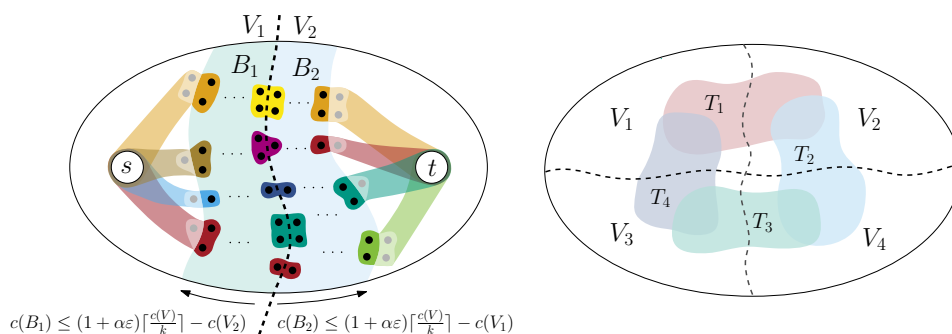
Input: Hypergraph $H = (V, E, c, \omega)$, k -way partition Π of H

```

1  $\mathcal{Q} \leftarrow \text{buildQuotientGraph}(H, \Pi)$  // see Section 5
2 while  $\exists$  active  $(V_i, V_j) \in \mathcal{Q}$  do in parallel // see Section 5
3    $B := B_i \cup B_j \leftarrow \text{constructRegion}(H, V_i, V_j)$  //  $B_i \subseteq V_i, B_j \subseteq V_j$ , see Section 6
4    $(\mathcal{N}, s, t) \leftarrow \text{constructFlowNetwork}(H, B)$  // see Section 6
5    $(M, \Delta_{\text{exp}}) \leftarrow \text{FlowCutterRefinement}(\mathcal{N}, s, t)$  // see Section 7 and 8
6   if  $\Delta_{\text{exp}} \geq 0$  // potential improvement
7      $\Delta_{\lambda-1} \leftarrow \text{applyMoves}(H, \Pi, M)$  // see Section 5
8     if  $\Delta_{\lambda-1} > 0$  mark  $V_i$  and  $V_j$  as active // found improvement
9     else if  $\Delta_{\lambda-1} < 0$  revertMoves}(H, \Pi, M) // no improvement

```

We first give an overview of how the different components in the framework interact with each other, before providing detailed component descriptions in their respective sections. For this we follow the high level structure of the algorithm, as shown in Algorithm 1. We start with a parallel scheduling scheme of block pairs based on the quotient graph in Section 5, see line 1 and 2. For each block pair, we extract a subhypergraph constructed around the boundary nodes of the blocks, which yields a flow network, see line 3 and 4 and Section 6. On each network we run the FlowCutter bipartitioning algorithm (line 5), whose partition we convert into a set of moves M and an expected connectivity reduction Δ_{exp} . FlowCutter and its parallelization are discussed in Section 7 and 8 respectively. If FlowCutter claims an improvement, i.e., $\Delta_{\text{exp}} > 0$, we apply the moves to the global partition and compute the exact reduction $\Delta_{\lambda-1}$, based on which we either mark the blocks for further refinement, or revert the moves, see line 8 and 9. We distinguish between expected and actual improvement, due to concurrency conflicts that arise in the scheduler, which is described again in Section 5. Finally, Section 9 describes the integration of the flow-based refinement routine into the shared-memory hypergraph partitioner Mt-KaHyPar [28, 30]. Note that Mt-KaHyPar provides data structures to concurrently access and modify the partition Π and the connectivity sets $\Lambda(e)$ and pin counts $\Phi(e, V_i)$ of each net $e \in E$ and block $V_i \in \Pi$ which we frequently use in the description of the following algorithms.



■ **Figure 1** Illustrates the flow network construction algorithm (left) and how we schedule block pairs of the quotient graph \mathcal{Q} in parallel (right, T_i denotes the search region of thread i).

5 Parallel Active Block Scheduling

Sanders and Schulz [54] propose the active block scheduling algorithm to apply their flow-based refinement algorithm for bipartitions on k -way partitions. Their algorithm proceeds in rounds. In each round, it schedules all pairs of adjacent blocks where at least one is marked as *active*. Initially, all blocks are marked as active. If a search on two blocks improves the edge cut, both are marked as active for the next round.

Parallelization. A simple parallelization scheme would be to schedule block pairs that form a maximum matching in the quotient graph \mathcal{Q} in parallel. This allows searches to operate in independent regions of the hypergraph and therefore not to conflict with each other. However, this scheme restricts the available parallelism to at most $\frac{k}{2}$ threads. Thus, we do not enforce any constraints on the block pairs processed concurrently, e.g., there can be multiple threads running on the same block and they can also share some of their nodes as illustrated in Figure 1 (right). This can lead to conflicts when we try to apply a move sequence found by a search on the partition Π and needs to be handled, which we discuss in detail in the next paragraph.

We use $\min(\min(t, \frac{k(k-1)}{2}), \tau \cdot k)$ threads to process the active block pairs in parallel, where t is the number of available threads in the system and $\frac{k(k-1)}{2}$ is the maximum number of adjacent blocks in the quotient graph \mathcal{Q} . The parameter τ controls the available parallelism in the scheduler. With higher values of τ , more block pairs are scheduled in parallel. This can lead to interference between searches that operate on similar regions. Lower values for τ can reduce these conflicts but put more emphasis on good parallelization of 2-way refinement to achieve good speedups.

Our parallel active block scheduling algorithm uses one global queue Q to schedule active block pairs. Each active block pair is associated with a round and each round uses an array of size k to mark blocks that become active in the next round. If a search finds an improvement on two blocks (V_i, V_j) and V_i or V_j becomes active, we push all its adjacent blocks into Q if they are not already contained in Q . If either V_i or V_j is already active, we insert (V_i, V_j) into Q if not contained. Thus, active block pairs of different rounds are stored interleaved in Q and the end of each round does not induce a synchronization point as in the original algorithm [54]. In the first round, we process all active block pairs in descending order of improvement they contributed on previous levels. On ties, we prefer block pairs with a larger number of cut hyperedges. A round ends when we have processed all its block pairs and all previous rounds have ended. If the relative improvement at the end of a round is less than 0.1%, we immediately terminate the algorithm.

Apply Moves. The flow-based refinement routine returns a move sequence M and the expected reduction Δ_{exp} in the connectivity metric when we apply M on the partition Π . Each move $m \in M$ is of the form $m = (u, V_i, V_j)$ or $m = (u, V_j, V_i)$ which means that node u is moved from block V_i to V_j or vice versa. If $\Delta_{\text{exp}} \geq 0$, we apply M on the partition Π . This may lead to conflicts, since applying M may invalidate some assumptions made by other threads about the partition Π or even the move sequence M itself may be based on some outdated information.

More precisely, there are three conflicts that can occur when we apply M . First, the move sequence leads to a partition that violates the balance constraint. Second, the actual improvement $\Delta_{\lambda-1}$ is not equal to the expected improvement Δ_{exp} . This is problematic when we actually degrade the solution quality. Finally, a node may be in a different block than expected by the move sequence. The algorithm that applies M is protected via a spin lock such that no other thread can modify the partition. In practice, the running time of this algorithm is negligible compared to solving the flow problem and is therefore not a sequential bottleneck (see Figure 8 in Section 10). We first remove all nodes from the sequence that are not in their expected block. Afterwards, we compute the block weights of the partition if all remaining moves were applied. We then perform the moves, if the resulting partition is balanced. During that, we compute the actual improvement $\Delta_{\lambda-1}$ of the move sequence. Suppose we move a node u from block V_i to V_j . For each net $e \in I(u)$, we add $\omega(e)$ to $\Delta_{\lambda-1}$, if $\Phi(e, V_i)$ decreases to zero and $-\omega(e)$ to $\Delta_{\lambda-1}$, if $\Phi(e, V_j)$ increases to one. If $\Delta_{\lambda-1} < 0$, we revert all moves.

Quotient Graph Construction. For each block pair, we explicitly store the hyperedges connecting the two. This information is required by the flow network construction algorithm which we describe in Section 6. Block pairs that contain at least one hyperedge form the edges of the quotient graph. We construct this data structure by iterating over all hyperedges in parallel and add a hyperedge $e \in E$ to the block pairs contained in $\{\{V_i, V_j\} \subseteq \Lambda(e) \mid i < j\}$.

If we apply a move sequence on the partition, we add all hyperedges $e \in E$ where $\Phi(e, V_j)$ increases to one to all block pairs contained in $\{\{V_j, V_k\} \mid V_k \in \Lambda(e) \setminus \{V_j\}\}$. If $\Phi(e, V_i)$ decreases to zero, we remove e lazily from corresponding block pairs during the flow network construction.

Implementation Details KaHyPar [33] established several pruning rules to skip unpromising flow computations that we also integrated into our framework. The first rule skips refinement on two adjacent blocks if the cut between both is less than ten (except on the finest level). The second rule modifies the active block scheduling algorithm such that after the first round only block pairs are scheduled where at least one computation on them improved the solution quality on a previous level.

We additionally introduce a time limit to abort long-running flow computations. During scheduling, we track the average running time \bar{t}_f required to solve a flow problem and set the time limit to $8 \cdot \bar{t}_f$. Note that we activate the time limit once k (number of blocks) block pairs have been processed.

6 Network Construction

To improve the cut of a bipartition $\Pi = \{V_1, V_2\}$, we grow a size-constrained region B around the cut hyperedges of Π . We then contract all nodes in $\bar{B}_1 := V_1 \setminus B$ to the source s and $\bar{B}_2 := V_2 \setminus B$ to the sink t [27, 54] as illustrated in Figure 1 (left) and obtain a coarser hypergraph \mathcal{H} . The flow network \mathcal{N} is then given by the Lawler expansion of \mathcal{H} (see

Section 2). Note that reducing the hyperedge cut of a bipartition induced by two adjacent blocks of a k -way partition Π_k optimizes the connectivity metric of Π_k [33].

Region Growing. Sanders and Schulz [54] grow a region $B := B_1 \cup B_2$ with $B_1 \subseteq V_1$ and $B_2 \subseteq V_2$ around the cut hyperedges of Π via two breadth-first-searches (BFS) as illustrated in Figure 1 (left). The first BFS is initialized with all boundary nodes of block V_1 and continues to add nodes to B_1 as long as $c(B_1) \leq (1 + \alpha\varepsilon)\lceil \frac{c(V_1)}{2} \rceil - c(V_2)$, where α is an input parameter. The second BFS that constructs B_2 proceeds analogously. For $\alpha = 1$, each flow computation yields a balanced bipartition with a possibly smaller cut in the original hypergraph, since only nodes of B can move to the opposite block ($c(B_1) + c(V_2) \leq (1 + \varepsilon)\lceil \frac{c(V_1)}{2} \rceil$ and vice versa). Larger values for α lead to larger flow problems with potentially smaller minimum cuts, but also increase the likelihood of violating the balance constraint. However, this is not a problem since the flow-based refinement routine guarantees balance through incremental minimum cut computations (see Section 7).

We additionally restrict the distance of each node $v \in B$ to the cut hyperedges to be smaller than or equal to a parameter δ . We observed that it is unlikely that a node *far* way from the cut is moved to the opposite block by the flow-based refinement.

Construction Algorithms. We implemented two construction algorithms that are preferable in different situations. Both construct the hypergraph \mathcal{H} as explained at the beginning of the section. In the following, we will denote with $E_B := \{e \in E \mid e \cap B \neq \emptyset\}$ the set of hyperedges that contain nodes of B .

The first algorithm iterates over all nets $e \in E_B$. If a pin $p \in e$ is contained in B , we add p to hyperedge e in \mathcal{H} . Otherwise, we add the source s or sink t to e , if $p \in V_1$ or $p \in V_2$. The complexity of the algorithm is $\mathcal{O}(\sum_{e \in E_B} |e|)$.

The second algorithm iterates over all nodes $u \in B$ and for each net $e \in I(u)$, we insert a pair (e, u) into a vector. Sorting the vector (lexicographically) yields the pin lists of the subhypergraph H_B . Afterwards, we insert each net e in the pin list vector into \mathcal{H} and add the source s or sink t to e , if $\Phi(e, B_1) < \Phi(e, V_1)$ or $\Phi(e, B_2) < \Phi(e, V_2)$. The complexity of the algorithm is $\mathcal{O}(p \log p)$ where $p := \sum_{e \in E_B} |e \cap B|$ is the number of pins of \mathcal{H} .

The first algorithm has linear running time, but has to scan all hyperedges of H in their entirety even if most of their pins are not contained in \mathcal{H} . The complexity of the second algorithm only depends on the number of pins in \mathcal{H} , but requires to sort the pin list vector. We use the second algorithm for hypergraphs with a low density $d := |E|/|V|$ (≤ 0.5) or a large average hyperedge size $\overline{|e|}$ (≥ 100).

Note that both algorithms discard single-pin nets and nets that contain both the source and sink (such nets cannot be removed from the cut).

Parallelization. The first algorithm iterates over all nets $e \in E_B$ in parallel and each thread uses the sequential algorithm to construct a thread-local pin list vector. Afterwards, we use a prefix sum operation to copy the pin lists of each thread to \mathcal{H} .

The second algorithm iterates over all nodes $u \in B$ in parallel and then uses hashing to distribute the pairs (e, u) to buckets. Afterwards, we process each bucket in parallel and apply the sequential algorithm to construct the pin list vector of each bucket. Finally, we use a prefix sum operation to copy the pin lists of each bucket to \mathcal{H} .

Identical Net Removal. Since some nets of H are only partially contained in \mathcal{H} , some of them may become identical. Therefore, we further reduce the size of \mathcal{H} by removing all identical nets except for one representative at which we aggregate their weight. We use the identical net detection algorithm of Aykanat et al. [8, 18]. It uses *fingerprints* $f_e := \sum_{v \in e} v^2$ to eliminate unnecessary pairwise comparisons between nets. Nets with different fingerprints

or different sizes cannot be identical. If we insert a net e into \mathcal{H} , we store the pair (f_e, e) in a hash table with chaining to resolve collisions (uses concurrent vectors to handle parallel access). We can then use the hash table to perform pin-list comparisons between the nets with the same fingerprint for subsequent net insertions. Note that in the parallel scenario we may not be able to detect all identical nets due to simultaneous insertions into the hash table. However, this does not affect correctness of the refinement, as removing identical nets is only a performance optimization.

7 Flow-Based Refinement

In this section we discuss the flow-based refinement routine on a bipartition. We first introduce the aforementioned FlowCutter algorithm [32, 60], which is used as the flow-based refinement routine in KaHyPar [26]. The algorithm is parallelized by plugging in a parallel maximum flow algorithm, which we discuss in detail in the next section. To speed up FlowCutter's convergence and to ensure there is sufficient work to make a parallel algorithm worthwhile, we propose an optimization named *bulk piercing*.

Core Algorithm. FlowCutter solves a sequence of incremental maximum flow problems until a balanced bipartition is found. Algorithm 2 shows pseudocode for the approach. In each iteration, first the previous flow (initially zero) is augmented to a maximum flow regarding the current source set S and sink set T , see line 3. Subsequently, the node sets $S_r, T_r \subset \mathcal{V}$ of the source- and sink-side cuts are derived in line 4. This is done via residual BFS (forward from S for S_r , backward from T for T_r). The node sets induce two bipartitions $(S_r, \mathcal{V} \setminus S_r)$ and $(\mathcal{V} \setminus T_r, T_r)$. If neither is balanced, all nodes on the side with smaller weight are transformed to a source (if $c(S_r) \leq c(T_r)$) or a sink otherwise, see lines 7-10. To find a different cut in the next iteration, one additional node is added, called *piercing node*. Thus, the bipartitions contributed by the currently smaller side will be more balanced in future iterations. Since the smaller side is grown, this process will converge to a balanced partition.

Algorithm 2 FlowCutter Core

```

1  $S \leftarrow \{s\}, T \leftarrow \{t\}$ 
2 while true do
3   augment flow to maximality regarding  $S, T$ 
4   derive source- and sink-side cut  $S_r, T_r \subset \mathcal{V}$ 
5   if  $(S_r, \mathcal{V} \setminus S_r)$  or  $(\mathcal{V} \setminus T_r, T_r)$  balanced
6     | return balanced partition
7   if  $c(S_r) \leq c(T_r)$ 
8     |  $S \leftarrow S_r \cup \text{selectPiercingNode}()$ 
9   else
10  |  $T \leftarrow T_r \cup \text{selectPiercingNode}()$ 

```

Piercing. Selecting a good piercing node is important to achieve good quality, which is why several selection heuristics were proposed. For our purpose, two heuristics are relevant: *avoiding augmenting paths* [32, 60] and *distance from cut* [26]. Whenever possible, a node that is not reachable from the source or sink should be picked, i.e., $v \in \mathcal{V} \setminus (S_r \cup T_r)$. Such nodes do not create an augmenting path, and thus the weight of the cut does not increase, while improving balance. As a secondary criterion, the distance from the original cut is used

(larger is better), to prefer reconstructing parts of the original cut over randomized decisions. This heuristic is only applicable in the refinement setting.

Most Balanced Cut. Once the partition is balanced, we try to improve the balance even further by continuing to pierce as long as no augmenting path is created. This process is repeated several times with different randomized choices since this is fast (no flow augmentation), starting from the first balanced partition. More balance gives other refinement algorithms more leeway for improvement. An equivalent heuristic was already employed in previous flow-based refinement approaches [52, 54].

Bulk Piercing. The complexity of FlowCutter is $O(\zeta m)$, where ζ is the final cut weight, and $m = |\mathcal{E}|$. This bound stems from a pessimistic implementation that augments one flow unit in $O(m)$ work [32, 60]. For refinement, the performance is much better in practice, as the first cut is often close to the final cut. Only few augmenting iterations are needed and much less than $O(m)$ work is spent per flow unit [27], with most work spent on the initial flow.

Still, the flow augmented per iteration is often small: at most the capacity of edges incident to the piercing node. On large instances, we observed that the number of required iterations increases substantially. We propose to accelerate convergence by piercing multiple nodes per iteration, as long as we cannot avoid augmenting paths and are far from balance. To ensure a poly-log iteration bound, we set a geometrically shrinking goal of weight to add to each side per iteration. The initial goal for the source side is set to $\beta(\frac{c(\mathcal{V})}{2} - c(s))$, where $\beta \in (0, 1)$ is the geometric shrinking factor that is multiplied with the term in each iteration, and $\frac{c(\mathcal{V})}{2} - c(s)$ is the weight to add for perfect balance.

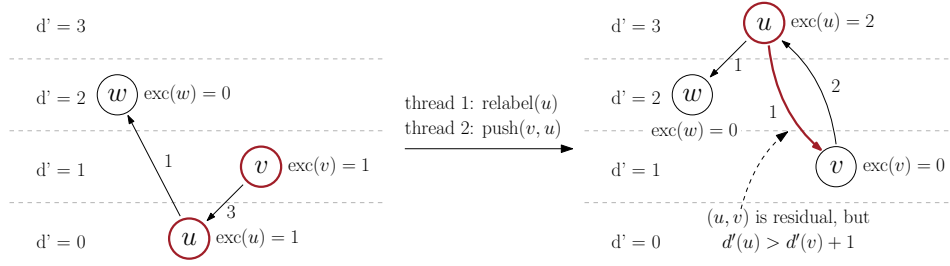
If a goal is not met, its remainder is added to next iteration’s goal. We track the average weight added per node and from this estimate the number of piercing nodes needed to match the current goal. To boost measurement accuracy, we pierce one node for the first few rounds. The sides have distinct measurements and goals, so that we do not pierce too aggressively when the smaller side flips. This scheme (with $\beta = 0.55$) reduces running time on our largest instances from beyond two hours (time limit) to less than 10 minutes, while not incurring any quality penalties on either small or large instances, as shown in our experiments.

8 Parallel Maximum Flow Algorithm

The maximum flow problem is log-space complete for P [25], i.e., the existence of a poly-log depth algorithm is unlikely. Furthermore, practical algorithms are notoriously difficult to parallelize efficiently [6, 10, 37, 57] and often achieve only mediocre speedups. Push-relabel algorithms are the most amenable to parallelization [6, 10, 37]. We picked the synchronous parallel algorithm of Baumstark et al. [10] because it restricts the amount of parallel work less than a recent coloring-based algorithm [37] and does not seem to incur additional work when more threads are added as opposed to recent asynchronous algorithms [35]. The second property is particularly important to us because threads may arbitrarily join a running flow computation due to the work-stealing scheduler. We first outline their algorithm, then describe a so far undocumented bug followed by our fix, and conclude with implementation details and intricacies of using FlowCutter with preflows. A preflow already yields a minimum cut, which suffices for our purpose.

8.1 Synchronous Parallel Push-Relabel

The algorithm proceeds in rounds in which all active nodes are discharged in parallel. The flow is updated globally, the nodes are relabeled locally and the excess differences are aggregated



■ **Figure 2** Illustrates a push-relabel conflict in the parallel discharge routine (adapted from Ref. [37]). The numbers on the arcs denote their residual capacities.

in a second array using atomic instructions. After all nodes have been discharged, the distance labels d are updated to the local labels d' and the excess deltas are applied. The discharging operations thus use the labels and excesses from the previous round. This is repeated until there are no nodes with $\text{exc}(v) > 0$ and $d(v) < n$ left.

To avoid concurrently pushing flow on residual arcs in both directions (race condition on flow values), a deterministic winning criterion on the old distance labels is used to determine which direction to push, if both nodes are active. If a node has an admissible arc it cannot push due to this, it may not be relabeled this round. Its discharging terminates after finishing the ongoing scan of residual arcs.

The rounds are interleaved with global relabeling [14], after linear push and relabel work, using parallel reverse BFS.

8.2 A Bug in the Synchronous Algorithm

The parallel discharge routine does not protect against push-relabel conflicts [37] as illustrated in Figure 2. In particular the winning criterion does not help. A node u may be relabeled too high if it is concurrently pushed to through a residual arc (v, u) with $d'(v) = d(u) + 1$. The arc (u, v) may not be observed as residual yet, and thus u may set its new label $d'(u) > d'(v) + 1$, violating label correctness. The bug becomes noticeable when the algorithm terminates prematurely with incorrect distances.

We propose two alternative fixes. The first is an atomic blocking mechanism, where active nodes are prohibited from being relabeled after being pushed to and prohibited from being pushed to after being relabeled in the same round; whichever operation comes first. The second fix is to collect mislabeled excess nodes during global relabeling. When the algorithm would terminate (no active nodes remaining), we run global relabeling, and restart the main loop if new active nodes were found.

We experimentally compare the two methods in Appendix D, finding that they perform equivalently well for plain flow computations. This is because the bug occurs quite rarely, and with the collection of mislabeled excess nodes in intermediate global relabeling steps, the final global relabeling is actually never necessary on our benchmark instances. For FlowCutter, however, we need the cuts, not just the flow assignment. Finding the sink-side cut can be done jointly with running the last global relabeling, so its work is already accounted for. Therefore, we chose this method.

8.3 Implementation Details

To facilitate an efficient, practical code, we discuss several implementation details. This covers techniques specific to the hypergraph setting, multi-source multi-sink settings and general techniques.

Restricting Capacities. Recall that only bridge edges $(e_{\text{in}}, e_{\text{out}})$ have finite capacity $(\omega(e))$ in the Lawler network. Since $(e_{\text{in}}, e_{\text{out}})$ is the only outgoing edge of e_{in} with non-zero capacity, the flow (but not preflow) on edges (u, e_{in}) is also bounded by $\omega(e)$. Adding these capacities during the preflow stage is a trivial optimization, but it reduces running time for one flow computation on our largest instance from over two hours to 14 seconds, when using 16 cores. It also boosts the available parallel work, since hypernodes are not immediately relieved of all their excess. Without this optimization the minimum cut contains only bridge edges, but now may contain edges (u, e_{in}) . This matters when tracking cut hyperedges (for collecting piercing candidates), which are detected by checking if e_{in} and e_{out} are on different sides. Therefore, we do not check the capacity and visit e_{in} nodes during forward residual BFSs.

Avoid Pushing Flow Back. Once the correct flow value is found, the algorithm could terminate in theory. This is often achieved in very few discharging rounds ($< 1\%$). Furthermore, we observed that the number of active nodes follows a power law distribution.

At this point flow is only pushed back to the source. We terminate once all nodes with $\text{exc}(u) > 0$ have $d(u) \geq n$, which is most often detected by global relabeling. Due to little work per round, it takes many rounds to trigger. We perform additional relabeling, if the flow value has not changed for some rounds (500), and only few active nodes (< 1500) were available in each. Since we expect to terminate, we also set markers for T_r .

Active Nodes. The set of active nodes is implemented as an array containing the nodes and an array of insertion timestamps that are atomically set to avoid duplicates. Nodes are accumulated in thread-local buffers that are frequently flushed to the shared array. During discharging, we build the array for the next round. We insert a node if it gets pushed to, or if it has excess left after its discharge operation. After a round of discharging, we swap the previous active nodes array with the newly built one, and increment the timestamp to reset the markers.

These arrays are reused for global relabeling as well as deriving the source-side and sink-side cuts. This enables computing the cut-side weights via a simple parallel reduction over the respective arrays, which we use to decide which side to grow.

Flow Value. We track the flow value to abort the refinement in case it exceeds the previous cut. Traditionally in push-relabel algorithms, the flow value is determined from the excess of the sink. Since we have many sinks, we do not want to repeatedly accumulate all of their excesses. Instead, we also insert sinks into the active nodes for the next round. This way, we can add their excess deltas to the flow value during the update phase, but we of course do not discharge them in the next round.

Hypergraph Implementation. For performance reasons we implement the flow algorithm directly on the hypergraph, simulating the Lawler expansion without actually constructing the graph flow network. We implement three separate discharge operations that scan the pins plus the bridge edge (in-node and out-node) or the incident hyperedges of a hypernode and push the appropriate amount of flow. The performance impact of this is demonstrated experimentally in Appendix D. While it is not as drastic as for Dinitz, where better optimizations are possible [26, 27], it is still worthwhile.

8.4 Intricacies with Preflows and FlowCutter

In this section, we discuss (some unexpected) challenges we faced during the implementation that arose from using FlowCutter with preflows. The major difference to actual flows is that there are nodes with positive excess left.

Source-Side Cut. First, note that a preflow only yields a sink-side cut via the reverse residual BFS, but for FlowCutter we also need the source-side cut. We can run a flow decomposition algorithm [14] to push excess back to the source, to obtain an actual flow and then compute it via forward residual BFS. However, flow decomposition is difficult to parallelize [10]. Instead, we initialize the forward residual BFS with all non-sink excess nodes. This finds the reverse paths that carry flow from the source to the excess nodes, which is precisely what we need.

Sink-Side Piercing. When transforming a node with positive excess to a sink, its excess must be added to the flow value. Fortunately, this only happens when piercing, as sink-side nodes have no excess if they are not sinks yet.

Maintain Distance Labels. Ideally, we want to reuse the distance labels to avoid re-initialization overheads. However, as the labels are a lower bound on the distance from the sink, piercing on the sink side invalidates the labels. Additionally, no new excess nodes are created. In this case, we run global relabeling to collect the existing excess nodes, before starting the main discharge loop. When piercing on the source side, new excesses are created, so we do not run the additional global relabel. Instead, we collect the existing excess nodes during regular runs; at the latest for the termination check.

9 Integration into a Multilevel Framework

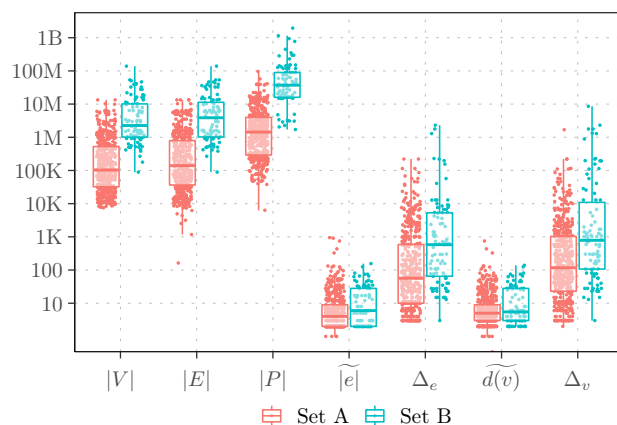
We integrated our flow-based refinement algorithm in the shared-memory multilevel partitioner Mt-KaHyPar. The framework provides two multilevel partitioners: one opts for the traditional $\mathcal{O}(\log n)$ level approach by contracting a vertex clustering on each level (Mt-KaHyPar-D [30]) and one implements a parallel version of the n -level scheme [49, 56, 56] that (un)contracts only a single vertex on each level (Mt-KaHyPar-Q [28]).

In each refinement step, Mt-KaHyPar-D first runs label propagation refinement [53] followed by FM local search [22]. We run our flow-based refinement as the third component. Mt-KaHyPar-Q uncontracts a fixed number of nodes on each level and then performs a highly-localized variant of label propagation and FM refinement. Using our flow-based refinement as a third technique would incur too much overhead, since there are $\mathcal{O}(|V|)$ levels and refinement steps. Thus, we use approximately $\mathcal{O}(\log n)$ synchronization points similar to Mt-KaHyPar-D and perform FM local search followed by our flow-based refinement. We do not run label propagation here since there were no quality benefits. We run all refinement algorithms on each level multiple times in combination and stop if the relative improvement is less than 0.25%.

10 Experiments

We implemented the flow-based refinement routine in the shared-memory hypergraph partitioner Mt-KaHyPar¹, which is implemented in C++17, parallelized using the TBB library [51], and compiled using g++9.2 with the flags `-O3 -mtune=native -march=native`. Mt-KaHyPar provides two partitioners: Mt-KaHyPar-D (Default setting) and Mt-KaHyPar-Q (Quality setting). We refer to the corresponding versions that use flow-based refinement as Mt-KaHyPar-D-F and Mt-KaHyPar-Q-F (-Flows). For parallel partitioners we add a suffix to

¹ Mt-KaHyPar is available from <https://github.com/kahypar/mt-kahypar>



■ **Figure 3** Summary of different properties for our two benchmark sets. It shows for each hypergraph (points), the number of vertices $|V|$, nets $|E|$ and pins $|P|$, as well as the median and maximum net size ($|e|$ and Δ_e) and vertex degree ($\widetilde{d}(v)$ and Δ_v).

their name to indicate the number of threads used, e.g. Mt-KaHyPar-Q-F 64 for 64 threads. We omit the suffix for sequential partitioners.

Instances. All instances of the benchmark sets used in the experimental evaluation are derived from four sources encompassing three application domains: the ISPD98 VLSI Circuit Benchmark Suite [3], the DAC 2012 Routability-Driven Placement Contest [59], the SuiteSparse Matrix Collection [16], and the 2014 SAT Competition [11]. VLSI instances are transformed into hypergraphs by converting the netlist of each circuit into a set of hyperedges. Sparse matrices are translated to hypergraphs using the row-net model [13] and SAT instances to three different hypergraph representations: *literal*, *primal*, and *dual* [48, 50] (see [34] for more details). All hypergraphs have unit vertex and net weights.

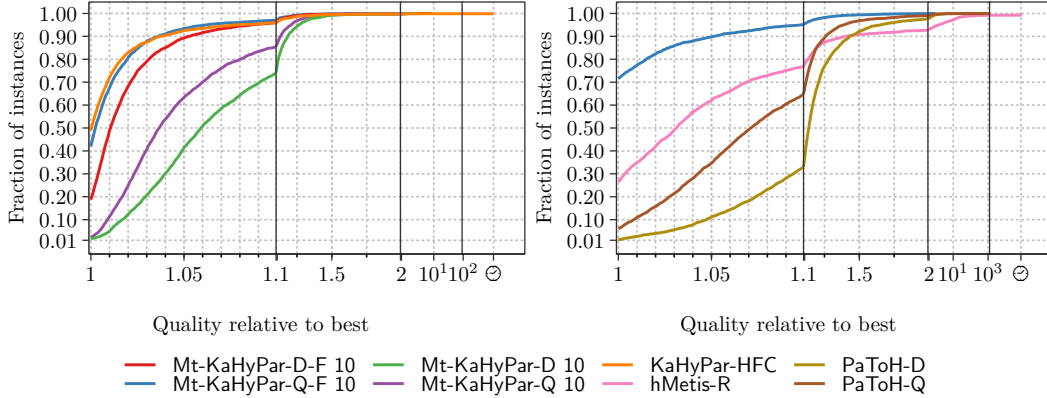
For comparison with sequential partitioners, we use the established benchmark set of Heuer and Schlag [34] (referred to as set A, 488 hypergraphs). To measure speedups and to compare our implementation with other parallel partitioners, we use a benchmark set composed of 94 large hypergraphs (referred to as set B) that was initially assembled to evaluate Mt-KaHyPar-D [30]. Figure 3 shows that the hypergraphs of set B are more than an order of magnitude larger than those of set A².

Setup. On set A, we use $k \in \{2, 4, 8, 16, 32, 64, 128\}$, $\varepsilon = 0.03$, ten different seeds and a time limit of eight hours. The experiments are done on a cluster of Intel Xeon Gold 6230 processors (2 sockets with 20 cores each) running at 2.1 GHz with 96GB RAM (machine A).

On set B, we use $k \in \{2, 8, 16, 64\}$, $\varepsilon = 0.03$, three seeds, and a time limit of two hours. These experiments are run on an AMD EPYC Rome 7702P (1 socket with 64 cores) running at 2.0–3.35 GHz with 1024GB RAM (machine B). The parameter space on set B is restricted, since we only have access to one machine of type B.

Methodology. Each partitioner optimizes the connectivity metric, which we also refer to as the quality of a partition. For each instance (hypergraph and k), we aggregate running times using the arithmetic mean over all seeds. To further aggregate over multiple instances, we use the geometric mean for absolute running times and self-relative speedups. For runs that

² The benchmark sets and experimental results are available from <https://algo2.iti.kit.edu/heuer/sea22>



■ **Figure 4** Performance profiles comparing solution quality of Mt-KaHyPar-Q-F with different partitioners on set A.

exceeded the time limit, we use the time limit itself in the aggregates. In plots, we mark these instances with \ominus if *all* runs of that algorithm timed out.

To compare the solution quality of different algorithms, we use *performance profiles* [21]. Let \mathcal{A} be the set of algorithms we want to compare, \mathcal{I} the set of instances, and $q_A(I)$ the quality of algorithm $A \in \mathcal{A}$ on instance $I \in \mathcal{I}$. For each algorithm A , we plot the fraction of instances (y -axis) for which $q_A(I) \leq \tau \cdot \min_{A' \in \mathcal{A}} q_{A'}(I)$, where τ is on the x -axis. Achieving higher fractions at lower τ -values is considered better. For $\tau = 1$, the y -value indicates the percentage of instances for which an algorithm performs best.

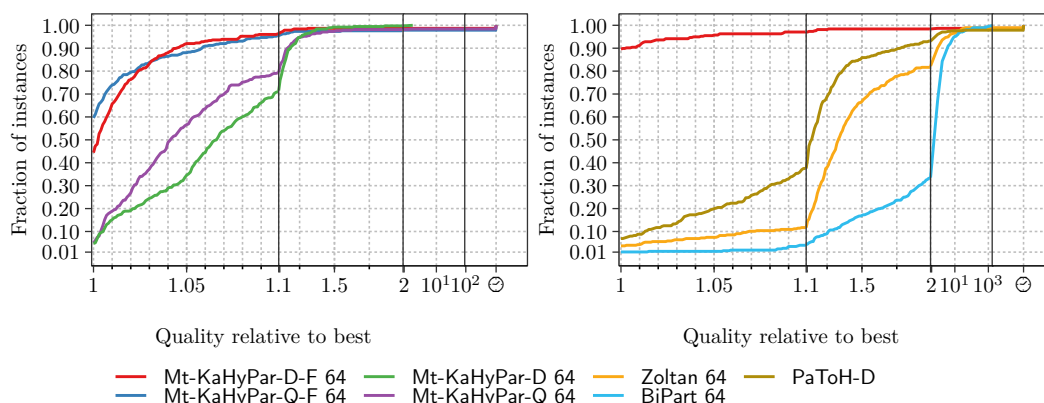
Parameter Configuration. We performed extensive parameter tuning experiments which we summarize in detail in Appendix A. The scheduler uses $\min(t, k)$ threads ($\tau = 1$) to process adjacent blocks of the quotient graph in parallel. We also enable bulk piercing as it has no impact on the solution quality while being consistently faster, with the geometric shrinking factor β set to 0.55. Further, we restrict the distance of each node to the cut hyperedges when we grow the region B to be smaller than or equal to $\delta = 2$. Finally, we set the region scaling parameter $\alpha = 16$ which is also used in the flow-based refinement algorithm of KaHyPar [33].

10.1 Comparison with other Algorithms

We now compare different partitioners with Mt-KaHyPar when using flow-based refinement. Since performance profiles do not permit a full ranking of three or more algorithms, we additionally add pairwise comparisons of Mt-KaHyPar-Q-F and all evaluated partitioners using performance profiles in Appendix B.

Medium-Sized Instances. On set A, we compare Mt-KaHyPar to KaHyPar-HFC [27, 33] (uses similar algorithmic components as Mt-KaHyPar-Q-F) which is the current best sequential partitioner in terms of solution quality [55], the recursive bipartitioning version (hMetis-R) of hMetis 2.0 [38], as well as the default (PaToH-D) and quality preset (PaToH-Q) of PaToH 3.3 [13]. All configurations of Mt-KaHyPar use 10 threads.

Figure 4 and 6 (left) compare the solution quality and running times of Mt-KaHyPar with different partitioners on set A. In an individual comparison, Mt-KaHyPar-Q-F finds better partitions than PaToH-D, PaToH-Q, Mt-KaHyPar-D, Mt-KaHyPar-Q, Mt-KaHyPar-D-F,



■ **Figure 5** Performance profiles comparing solution quality of Mt-KaHyPar-D-F with different partitioners on set B.

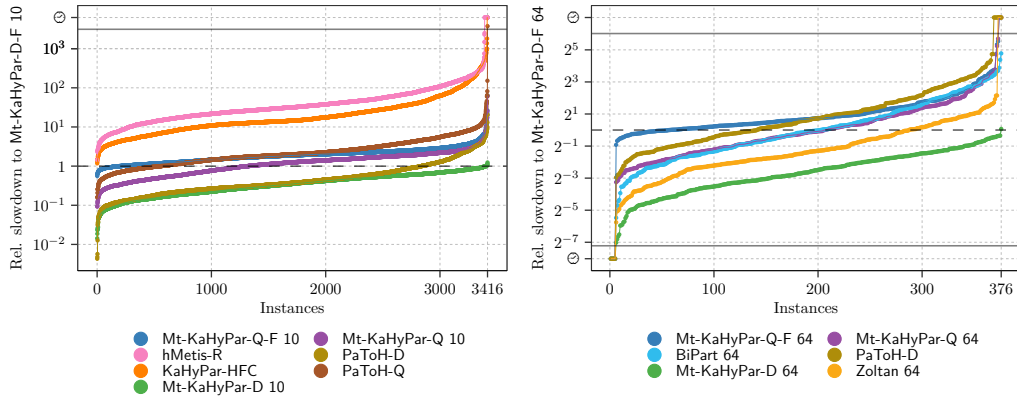
hMetis-R and KaHyPar-HFC on 94.7%, 87.7%, 97.3%, 95.7%, 73.5%, 74.5% and 51.3% of the instances, respectively.

The median improvement of Mt-KaHyPar-D-F and Mt-KaHyPar-Q-F compared to the configurations that use no flow-based refinement is 4.2% and 2.7% while only incurring a slowdown by a factor of 3.1 (gmean time 2.73s vs 0.89s) and 1.7 (5.08s vs 2.99s). To put this into perspective, the quality preset of PaToH (PaToH-Q) improves the default preset (PaToH-D) by 5.3% in the median and is a factor of 5 slower (5.86s vs 1.17s). The median improvement of hMetis-R compared to PaToH-Q is 2.6% while it is a factor of 15.9 slower (93.21s vs 5.86s). The solutions produced by Mt-KaHyPar-Q-F are 3% better than those of hMetis-R in the median and it has a similar running time as PaToH-Q (5.08s vs 5.86s). If we compare our two partitioners that use flow-based refinement (see also Figure 14 in Appendix B), we can see that Mt-KaHyPar-Q-F gives only minor quality improvements over Mt-KaHyPar-D-F (median improvement is 0.6% whereas without flow-based refinement it is 1.9%). This demonstrates the effectiveness of flow-based refinement. The solution quality of Mt-KaHyPar-Q-F and KaHyPar-HFC are on par (see also Figure 14 in Appendix B), while Mt-KaHyPar-Q-F is an order of magnitude faster with 10 threads (5.08s vs 48.98s). In conclusion, we achieved the solution quality of the currently highest quality sequential partitioner in a fast parallel code.

Large Instances. On set B, we compare Mt-KaHyPar with the parallel algorithms Zoltan 3.83 [19] and BiPart [47], as well as PaToH-D, which is the only sequential algorithm to complete the experiments in a reasonable time frame. All parallel algorithms use 64 threads.

Figure 5 and 6 (right) compare the solution quality and running times of Mt-KaHyPar with different partitioners on set B. The quality of the partitions produced by Mt-KaHyPar-D-F and Mt-KaHyPar-Q-F are comparable (see also Figure 15 in Appendix B) while Mt-KaHyPar-D-F is a factor of 1.9 faster (gmean time 30.38s vs 58.24s). Therefore, we focus on Mt-KaHyPar-D-F in this evaluation. In an individual comparison, Mt-KaHyPar-D-F finds better partitions than BiPart, Zoltan, PaToH-D, Mt-KaHyPar-D, Mt-KaHyPar-Q and Mt-KaHyPar-Q-F on 97.3%, 96%, 92%, 91%, 85.1% and 47.3% of the instances, respectively.

The median improvement of Mt-KaHyPar-D-F and Mt-KaHyPar-Q-F compared to the configurations that use no flow-based refinement is 5.2% and 3.4% while they are slower by a factor of 6.6 (30.38s vs 4.63s) and 1.9 (58.24s vs 29.99s). Both the improvements and slowdowns are more pronounced here than on set A. The slowdowns are expected since the size of the flow problems scales linearly with instance sizes, while the complexity of the



■ **Figure 6** Running times relative to Mt-KaHyPar-D-F on set A (left) and B (right). The \ominus axis markers represent timeouts for the baseline Mt-KaHyPar-D-F (at the bottom) or the compared algorithm (at the top).

flow-based refinement routine does not. Mt-KaHyPar-D-F (30.38s) is slower than Zoltan (12.6s) and BiPart (29.19s), but faster than PaToH-D (50.3s). However, Mt-KaHyPar-D-F computes partitions that are 33% better than those of Zoltan and twice as good as those of BiPart in the median.

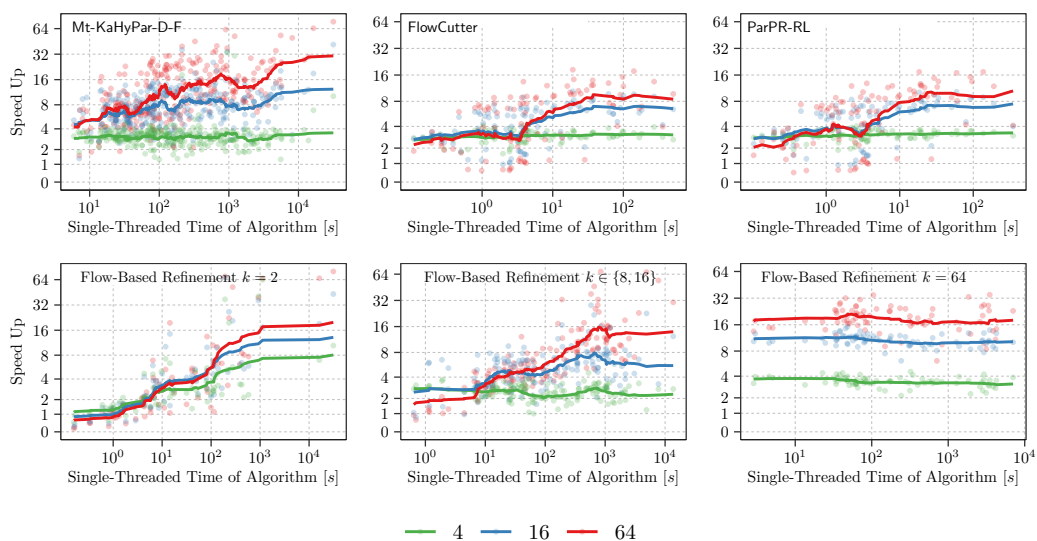
10.2 Scalability

In Figure 7, we summarize self-relative speedups for several algorithmic components of Mt-KaHyPar-D-F with varying number of threads $t \in \{4, 16, 64\}$. In the plot, we represent the speedup of each instance as a point and the centered rolling geometric mean with a window size of 25 as a line.

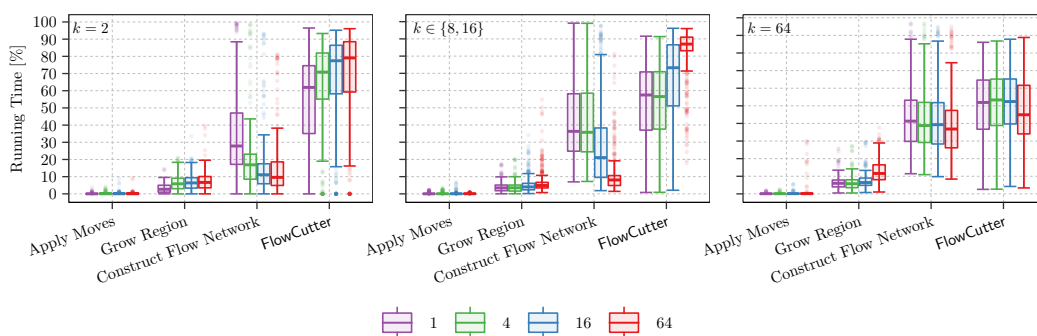
FlowCutter. To assess the scalability of FlowCutter and the flow algorithm ParPR-RL, we extract flow networks from bipartitions of the instances in set B. The instances are available on the website along the other benchmark instances. The results are shown in the top middle and right plots of Figure 7. With 4 threads, we observe near-perfect speedups throughout, with fairly small variance. For $t = 16, 64$, the parallelization overheads are only outweighed for longer running instances, with more threads becoming worthwhile at about 10 seconds of sequential time. Unfortunately, we even experience some minor slowdowns and the speedups are strongly scattered. The maximum achieved speedups are 10.4, 18.4 for FlowCutter and 10.3, 17.3 for ParPR-RL. These results match what we expected from [10]. Restricted to instances with sequential running time ≥ 10 seconds, the geometric mean speedups are 6.5 and 8.6 for FlowCutter and 7, 9.9 for ParPR-RL.

Mt-KaHyPar. We run the scalability experiments for Mt-KaHyPar-D-F on a subset of set B (76 out of 94 hypergraphs) that contains all hypergraphs on which Mt-KaHyPar-D-F 64 was able to complete in under 600 seconds for all $k \in \{2, 8, 16, 64\}$ ³. We omit scalability experiments with Mt-KaHyPar-Q-F due to the long time requirements and because flow-based refinement is used in the same context in Mt-KaHyPar-D-F. Note that we use sequential implementations of the flow network construction and maximum flow algorithm in case the number of flow problems processed in parallel is equal to the number of available threads.

³ This experiment still took 4 weeks on machine B



■ **Figure 7** Speedups of Mt-KaHyPar-D-F and the flow-based refinement routine (for different values of k) as well as of the FlowCutter and parallel flow algorithm (ParPR-RL).

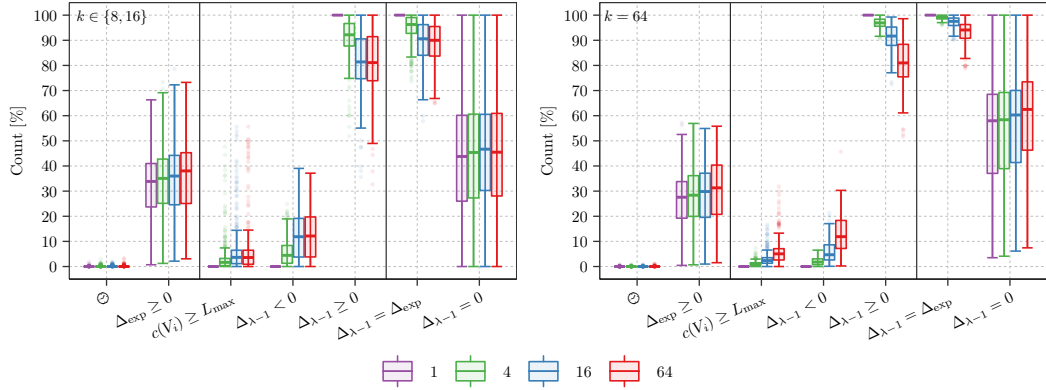


■ **Figure 8** Running times of the different phases of the flow-based refinement routine relative to its total running time for $k = 2$ (left), $k \in \{8, 16\}$ (middle) and $k = 64$ (right) on set B.

Hence, scalability is limited by parallelization overheads and memory bandwidth, which makes achieving perfect speedups difficult.

The overall geometric mean speedup of Mt-KaHyPar-D-F is 3.1 for $t = 4$, 7.4 for $t = 16$ and 10.62 for $t = 64$. If we only consider instances with a single-threaded running time ≥ 100 s, we achieve a geometric mean speedup of 14.5 for $t = 64$.

For $k = 2$, the scalability of the flow-based refinement routine largely depends on FlowCutter as the only parallelism source. We can see that the speedups of the two are comparable (compare Figure 7 top-middle with bottom-left). There are a few outliers (e.g. `nlpkkt200` with a speedup of 80.05 for $t = 64$) where the flow network construction dominates the overall execution time for $t = 1$. For $k = 64$ and $t = 64$, we achieve a geometric mean speedup of 18.48. In this case, all parallelism is leveraged in the scheduler, and none in FlowCutter, which explains why we obtain more reliable speedups than for all other k . As the outer parallel construct, the scheduler is the more amenable parallelism source. For $k \in \{8, 16\}$, both parallelism sources are used. The speedups are slightly better than for



■ **Figure 9** Conflicts for $k \in \{8, 16\}$ (left) and $k = 64$ (right) on set B. For each instance, we count the refinements that exceed the time limit (\ominus), the potential improvements ($\Delta_{\text{exp}} \geq 0$) and move sequences that violate the balance constraint ($c(V_i) \geq L_{\text{max}}$) or degrade ($\Delta_{\lambda-1} < 0$) or improve the connectivity metric ($\Delta_{\lambda-1} \geq 0$). For move sequences with $\Delta_{\lambda-1} \geq 0$, we count if the actual improvements equals the expected ($\Delta_{\lambda-1} = \Delta_{\text{exp}}$) and zero-gain improvements ($\Delta_{\lambda-1} = 0$).

$k = 2$. Note that the poor speedups for instances with short single-threaded running times (≤ 10 s) are caused by parallelization overheads of the network construction and maximum flow algorithm.

Figure 8 shows the running times of the different phases of the flow-based refinement routine relative to its total running time. For $k \leq 16$, FlowCutter dominates the running time. For $k = 64$, the flow network construction and FlowCutter have the same share on the total running time, while applying move sequences and growing the region B are negligible.

Search Interference. Figure 9 gives an overview on the different types of conflicts in the flow-based refinement routine (as explained in Section 5) and how often they occur. In the median, 33.38% of flow-based refinements find a potential improvement, of which we successfully apply 85.62% to the global partition for $t = 64$ (90.48% for $t = 16$ and 96.73% for $t = 4$). For $t = 64$, 2.55% of the move sequences violate the balance constraint (2% for $t = 16$ and 0.77% for $t = 4$) and 8.06% actually degrade the solution quality (4.74% for $t = 16$ and 1.72% for $t = 4$). However, increasing the number of threads does not adversely affect the solution quality of Mt-KaHyPar-D-F (see Figure 18 in Appendix C).

11 Conclusion and Future Work

This work marks the end of a series of publications with the aim to transfer techniques used in modern sequential partitioning algorithms into the shared-memory context without compromises in solution quality. The result is a set of parallel algorithms unified in one framework (Mt-KaHyPar) that outperforms all popular hypergraph partitioners [28, 30].

Summarizing our experimental results, we obtain good speedups for medium size values of k , where we can rely on the scheduler, and acceptable speedups for small k , where the parallelism stems from the maximum flow algorithm. Using 10 threads, our system is 10 times faster than the sequential state-of-the-art system KaHyPar with flow-based refinement, while achieving the same solution quality (connectivity metric).

Future work includes a deterministic version of parallel flow-based refinement to extend the existing deterministic algorithm [29], as well as a highly localized version used in the n -level partitioner [28] that only constructs small flow problems around uncontracted nodes.

References

- 1 Yaroslav Akhremtsev, Tobias Heuer, Peter Sanders, and Sebastian Schlag. Engineering a Direct k -way Hypergraph Partitioning Algorithm. In *19th Workshop on Algorithm Engineering & Experiments (ALENEX)*, pages 28–42. SIAM, 01 2017. doi:10.1137/1.9781611974768.3.
- 2 Yaroslav Akhremtsev, Peter Sanders, and Christian Schulz. High-Quality Shared-Memory Graph Partitioning. In *European Conference on Parallel Processing (Euro-Par)*, pages 659–671. Springer, 8 2017. doi:10.1007/978-3-319-96983-1_47.
- 3 Charles J. Alpert. The ISPD98 Circuit Benchmark Suite. In *International Symposium on Physical Design (ISPD)*, pages 80–85, 4 1998. doi:10.1145/274535.274546.
- 4 Charles J. Alpert and Andrew B. Kahng. Recent Directions in Netlist Partitioning: A Survey. *Integration*, 19(1-2):1–81, 1995. doi:10.1016/0167-9260(95)00008-4.
- 5 Reid Andersen. and Kevin J. Lang. An Algorithm for Improving Graph Partitions. In *Proc. of the 19th ACM-SIAM Symposium on Discrete Algorithms*, pages 651–660. Society for Industrial and Applied Mathematics, 2008. doi:10.5555/1347082.1347154.
- 6 Richard J. Anderson and João C. Setubal. A Parallel Implementation of the Push-Relabel Algorithm for the Maximum Flow Problem. *J. Parallel Distributed Comput.*, 29(1):17–26, 1995. doi:10.1006/jpdc.1995.1103.
- 7 Aaron Archer, Kevin Aydin, MohammadHossein Bateni, Vahab S. Mirrokni, Aaron Schild, Ray Yang, and Richard Zhuang. Cache-Aware Load Balancing of Data Center Applications. *Proceedings of the VLDB Endowment*, 12(6):709–723, 2019. doi:10.14778/3311880.3311887.
- 8 Cevdet Aykanat, Berkant Barla Cambazoglu, and Bora Uçar. Multi-level Direct k -way Hypergraph Partitioning With Multiple Constraints and Fixed Vertices. *Journal of Parallel and Distributed Computing*, 68(5):609–625, 2008. doi:10.1016/j.jpdc.2007.09.006.
- 9 David A. Bader, Henning Meyerhenke, Peter Sanders, and Dorothea Wagner. *Graph Partitioning and Graph Clustering*, volume 588. American Mathematical Society Providence, RI, 2013. doi:10.1090/conm/588.
- 10 Niklas Baumstark, Guy E. Blelloch, and Julian Shun. Efficient implementation of a synchronous parallel push-relabel algorithm. In Nikhil Bansal and Irene Finocchi, editors, *Algorithms - ESA 2015 - 23rd Annual European Symposium, Patras, Greece, September 14-16, 2015, Proceedings*, volume 9294 of *Lecture Notes in Computer Science*, pages 106–117. Springer, 2015. doi:10.1007/978-3-662-48350-3_10.
- 11 Anton Belov, Daniel Diepold, Marijn Heule, and Matti Järvisalo. The SAT Competition 2014. <http://www.satcompetition.org/2014/>, 2014.
- 12 Thang N. Bui and Curt Jones. A Heuristic for Reducing Fill-In in Sparse Matrix Factorization. In *6th SIAM Conference on Parallel Processing for Scientific Computing (PPSC)*, pages 445–452, 1993. URL: <https://www.osti.gov/biblio/54439>.
- 13 Ümit V. Catalyurek and Cevdet Aykanat. Hypergraph-Partitioning-based Decomposition for Parallel Sparse-Matrix Vector Multiplication. *IEEE Transactions on Parallel and Distributed Systems*, 10(7):673–693, 1999. doi:10.1109/71.780863.
- 14 Boris V. Cherkassky and Andrew V. Goldberg. On Implementing the Push-Relabel Method for the Maximum Flow Problem. *Algorithmica*, 19(4):390–410, 1997. doi:10.1007/PL00009180.
- 15 Carlo Curino, Yang Zhang, Evan P. C. Jones, and Samuel Madden. Schism: a Workload-Driven Approach to Database Replication and Partitioning. *Proceedings of the VLDB Endowment*, 3(1):48–57, 2010. doi:10.14778/1920841.1920853.

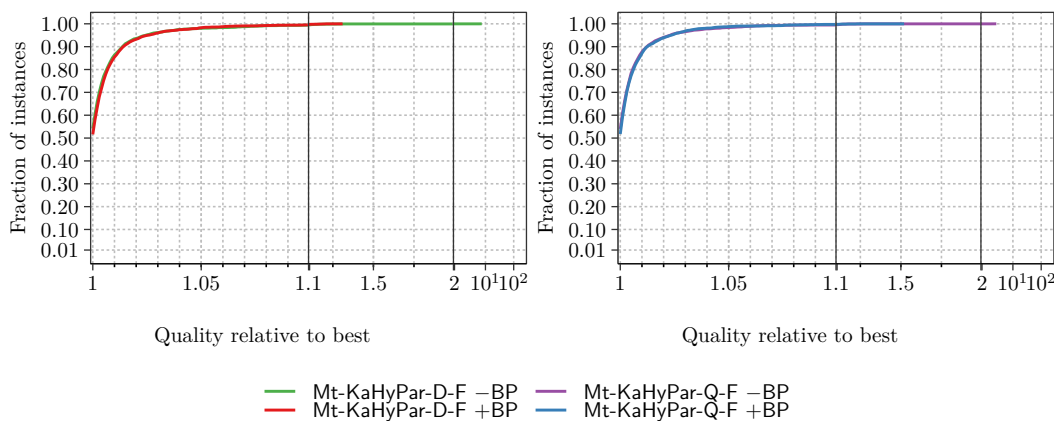
- 16 Timothy A. Davis and Yifan Hu. The University of Florida Sparse Matrix Collection. *ACM Transactions on Mathematical Software*, 38(1):1:1–1:25, 11 2011. doi:10.1145/2049662.2049663.
- 17 Daniel Delling, Andrew V. Goldberg, Ilya Razenshteyn, and Renato F. Werneck. Graph Partitioning with Natural Cuts. In *Proc. of the 25th International Parallel and Distributed Processing Symposium*, pages 1135–1146, 2011. doi:10.1109/IPDPS.2011.108.
- 18 Mehmet Deveci, Kamer Kaya, and Ümit V. Çatalyürek. Hypergraph Sparsification and Its Application to Partitioning. In *42nd International Conference on Parallel Processing, ICPP 2013, Lyon, France, October 1-4, 2013*, pages 200–209, 2013. doi:10.1109/ICPP.2013.29.
- 19 Karen D. Devine, Erik G. Boman, Robert T. Heaphy, Rob H. Bisseling, and Ümit V. Catalyurek. Parallel Hypergraph Partitioning for Scientific Computing. In *IEEE Transactions on Parallel and Distributed Systems*, pages 10–pp. IEEE, 2006. doi:10.1109/IPDPS.2006.1639359.
- 20 Yefim Dinitz. Algorithm for Solution of a Problem of Maximum Flow in a Network with Power Estimation. *Soviet Mathematics-Doklady*, 11(5):1277–1280, September 1970.
- 21 Elizabeth D. Dolan and Jorge J. Moré. Benchmarking Optimization Software with Performance Profiles. *Mathematical Programming*, 91(2):201–213, 2002. doi:10.1007/s101070100263.
- 22 Charles M. Fiduccia and Robert M. Mattheyses. A Linear-Time Heuristic for Improving Network Partitions. In *19th Conference on Design Automation (DAC)*, pages 175–181, 1982. doi:10.1145/800263.809204.
- 23 Lester Randolph Ford and Delbert R Fulkerson. Maximal Flow through a Network. *Canadian Journal of Mathematics*, 8:399–404, 1956. doi:10.4153/CJM-1956-045-5.
- 24 Andrew V. Goldberg and Robert Endre Tarjan. A New Approach to the Maximum-Flow Problem. *Journal of the ACM*, 35(4):921–940, 1988. doi:10.1145/48014.61051.
- 25 Leslie M. Goldschlager, Ralph A. Shaw, and John Staples. The Maximum Flow Problem is Log Space Complete for P. *Theoretical Computer Science*, 21:105–111, 1982. doi:10.1016/0304-3975(82)90092-5.
- 26 Lars Gottesbüren, Michael Hamann, Sebastian Schlag, and Dorothea Wagner. Advanced Flow-Based Multilevel Hypergraph Partitioning. *18th International Symposium on Experimental Algorithms (SEA)*, 2020. doi:10.4230/LIPIcs.SEA.2020.11.
- 27 Lars Gottesbüren, Michael Hamann, and Dorothea Wagner. Evaluation of a Flow-Based Hypergraph Bipartitioning Algorithm. In *27th European Symposium on Algorithms (ESA)*, pages 52:1–52:17, 2019. doi:10.4230/LIPIcs.ESA.2019.52.
- 28 Lars Gottesbüren, Tobias Heuer, Peter Sanders, and Sebastian Schlag. Shared-Memory n -level Hypergraph Partitioning. In *Workshop on Algorithm Engineering and Experiments (ALENEX)*. SIAM, 2022. to appear. URL: <https://arxiv.org/abs/2104.08107>.
- 29 Lars Gottesbüren and Michael Hamann. Deterministic parallel hypergraph partitioning. *CoRR*, abs/2112.12704, 2021. URL: <https://arxiv.org/abs/2112.12704>, arXiv:2112.12704.
- 30 Gottesbüren, Lars and Heuer, Tobias and Sanders, Peter and Schlag, Sebastian. Scalable Shared-Memory Hypergraph Partitioning. In *23st Workshop on Algorithm Engineering & Experiments (ALENEX)*. SIAM, 01 2021. doi:10.1137/1.9781611976472.2.
- 31 Johnnie Gray and Stefanos Kourtis. Hyper-optimized tensor network contraction. *Quantum*, 5:410, 2021. doi:10.22331/q-2021-03-15-410.
- 32 Michael Hamann and Ben Strasser. Graph Bisection with Pareto Optimization. *ACM Journal of Experimental Algorithmics*, 23, 2018. doi:10.1145/3173045.

- 33 Tobias Heuer, Peter Sanders, and Sebastian Schlag. Network Flow-Based Refinement for Multilevel Hypergraph Partitioning. *ACM Journal of Experimental Algorithmics (JEA)*, 24(1):2.3:1–2.3:36, 09 2019. doi:10.1145/3329872.
- 34 Tobias Heuer and Sebastian Schlag. Improving Coarsening Schemes for Hypergraph Partitioning by Exploiting Community Structure. In *16th International Symposium on Experimental Algorithms (SEA)*, pages 21:1–21:19. Schloss Dagstuhl – Leibniz-Zentrum für Informatik, 06 2017. doi:10.4230/LIPIcs.SEA.2017.21.
- 35 Bo Hong and Zhengyu He. An Asynchronous Multithreaded Algorithm for the Maximum Network Flow Problem with Nonblocking Global Relabeling Heuristic. *IEEE Transaction on Parallel Distributed Systems*, 22(6):1025–1033, 2011. doi:10.1109/TPDS.2010.156.
- 36 Igor Kabiljo, Brian Karrer, Mayank Pundir, Sergey Pupyrev, Alon Shalita, Yaroslav Akhremtsev, and Alessandro Presta. Social Hash Partitioner: A Scalable Distributed Hypergraph Partitioner. In *Proceedings of the VLDB Endowment*, volume 10, pages 1418–1429, 2017. doi:10.14778/3137628.3137650.
- 37 Gökçehan Kara and Can C. Özturan. Graph Coloring Based Parallel Push-relabel Algorithm for the Maximum Flow Problem. *ACM Transactions on Mathematical Software*, 45(4):46:1–46:28, 2019. doi:10.1145/3330481.
- 38 George Karypis, Rajat Aggarwal, Vipin Kumar, and Shashi Shekhar. Multilevel Hypergraph Partitioning: Applications in VLSI Domain. *IEEE Transactions on Very Large Scale Integration (VLSI) Systems*, 7(1):69–79, 1999. doi:10.1109/92.748202.
- 39 George Karypis and Vipin Kumar. Multilevel k -way Hypergraph Partitioning. *VLSI Design*, 2000(3):285–300, 2000. doi:10.1155/2000/19436.
- 40 Alexander V. Karzanov. Determining the Maximal Flow in a Network by the Method of Preflows. In *Soviet Mathematics Doklady*, volume 15, pages 434–437, 1974.
- 41 Brian W. Kernighan and Shen Lin. An Efficient Heuristic Procedure for Partitioning Graphs. *The Bell System Technical Journal*, 49(2):291–307, 2 1970.
- 42 Balakrishnan Krishnamurthy. An improved min-cut algorithm for partitioning VLSI networks. *IEEE Trans. Computers*, 33(5):438–446, 1984. doi:10.1109/TC.1984.1676460.
- 43 Kevin J. Lang and Satish Rao. A Flow-Based Method for Improving the Expansion or Conductance of Graph Cuts. In *Proc. of 10th International Integer Programming and Combinatorial Optimization Conference*, volume 3064 of *LNCS*, pages 383–400. Springer, 2004. doi:10.1007/978-3-540-25960-2_25.
- 44 Dominique LaSalle and George Karypis. Multi-Threaded Graph Partitioning. In *IEEE Transactions on Parallel and Distributed Systems*, pages 225–236. IEEE, 2013. doi:10.1109/IPDPS.2013.50.
- 45 Eugene L. Lawler. Cutsets and Partitions of Hypergraphs. *Networks*, 3(3):275–285, 1973. doi:10.1002/net.3230030306.
- 46 Thomas Lengauer. *Combinatorial Algorithms for Integrated Circuit Layout*. John Wiley & Sons, Inc., 1990. doi:10.1017/S0263574700015691.
- 47 Sepideh Maleki, Udit Agarwal, Martin Burtscher, and Keshav Pingali. BiPart: A Parallel and Deterministic Hypergraph Partitioner. In *Proceedings of the 26th ACM SIGPLAN Symposium on Principles and Practice of Parallel Programming*, pages 161–174, 2021. doi:10.1145/3437801.3441611.
- 48 Zoltán Á. Mann and Pál A. Papp. Formula Partitioning Revisited. In *5th Pragmatics of SAT Workshop*, pages 41–56, 2014. doi:10.29007/9skn.
- 49 Vitaly Osipov and Peter Sanders. n -Level Graph Partitioning. In *18th European Symposium on Algorithms (ESA)*, pages 278–289. Springer, 2010. doi:10.1007/978-3-642-15775-2_24.

- 50 David A. Papa and Igor L. Markov. Hypergraph Partitioning and Clustering. In *Handbook of Approximation Algorithms and Metaheuristics*. 2007. doi:10.1201/9781420010749.ch61.
- 51 Chuck Pheatt. Intel Threading Building Blocks. *Journal of Computing Sciences in Colleges*, 23(4):298–298, 2008.
- 52 Jean-Claude Picard and Maurice Queyranne. On the Structure of All Minimum Cuts in a Network and Applications. *Math. Program.*, 22(1):121, 1982. doi:10.1007/BF01581031.
- 53 Usha Nandini Raghavan, Réka Albert, and Soundar Kumara. Near Linear Time Algorithm to Detect Community Structures in Large-Scale Networks. *Physical Review E*, 76(3):036106, 2007. doi:10.1103/PhysRevE.76.036106.
- 54 Peter Sanders and Christian Schulz. Engineering Multilevel Graph Partitioning Algorithms. In *19th European Symposium on Algorithms (ESA)*, pages 469–480. Springer, 2011. doi:10.1007/978-3-642-23719-5_40.
- 55 Sebastian Schlag. High-Quality Hypergraph Partitioning. 2020. doi:10.5445/IR/1000105953.
- 56 Sebastian Schlag, Vitali Henne, Tobias Heuer, Henning Meyerhenke, Peter Sanders, and Christian Schulz. k -way Hypergraph Partitioning via n -Level Recursive Bisection. In *18th Workshop on Algorithm Engineering & Experiments (ALENEX)*, pages 53–67. SIAM, 2016. doi:10.1137/1.9781611974317.5.
- 57 Yossi Shiloach and Uzi Vishkin. An $O(n^2 \log n)$ Parallel Max-Flow Algorithm. *Journal of Algorithms*, 3(2):128–146, 1982. doi:10.1016/0196-6774(82)90013-X.
- 58 Aleksandar Trifunovic and William J. Knottenbelt. Parkway 2.0: A Parallel Multilevel Hypergraph Partitioning Tool. In *International Symposium on Computer and Information Sciences*, pages 789–800. Springer, 2004. doi:10.1007/978-3-540-30182-0_79.
- 59 Natarajan Viswanathan, Charles J. Alpert, Cliff C. N. Sze, Zhuo Li, and Yaoguang Wei. The DAC 2012 Routability-Driven Placement Contest and Benchmark Suite. In *49th Conference on Design Automation (DAC)*, pages 774–782. ACM, 6 2012. doi:10.1145/2228360.2228500.
- 60 Hannah Honghua Yang and D.F. Wong. Efficient Network Flow Based Min-Cut Balanced Partitioning. *IEEE Transactions on Computer-Aided Design of Integrated Circuits and Systems*, 15(12):1533–1540, 1996. doi:10.1007/978-1-4615-0292-0_41.

A Parameter Tuning

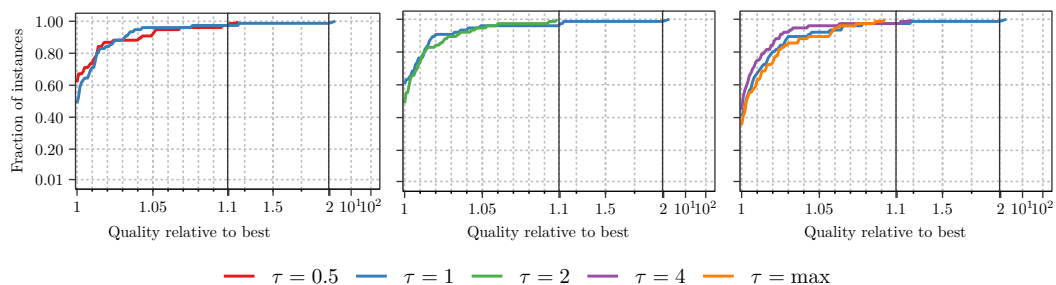
The flow-based refinement algorithm has several parameters whose choice influences the solution quality and running time of Mt-KaHyPar. This section summarizes our parameter tuning experiments and explains the tradeoffs that led to the final parameter configuration. We summarize the running times of all evaluated configurations in Table 1.



■ **Figure 10** Performance profiles comparing solution quality of Mt-KaHyPar-D-F and Mt-KaHyPar-Q-F with (+BP) and without bulk piercing (-BP) on set A.

Bulk Piercing. We evaluated the performance of the FlowCutter algorithm as flow-based refinement in Mt-KaHyPar with (+BP) and without bulk piercing (-BP). The experiments are conducted on set A and machine A with $k \in \{2, 4, 8, 16, 32, 64, 128\}$, $\varepsilon = 0.03$ and 10 repetitions. All configurations use 10 threads.

Figure 10 shows that there are no noticeable differences in solution quality when using bulk piercing. Furthermore, both variants that uses bulk piercing are slightly faster than their counterparts that only pierces one vertex in each iteration (gmean time 2.73s vs 2.96s, Mt-KaHyPar-D-F, and 5.08s vs 5.25s, Mt-KaHyPar-Q-F). Thus, we enable bulk piercing per default.

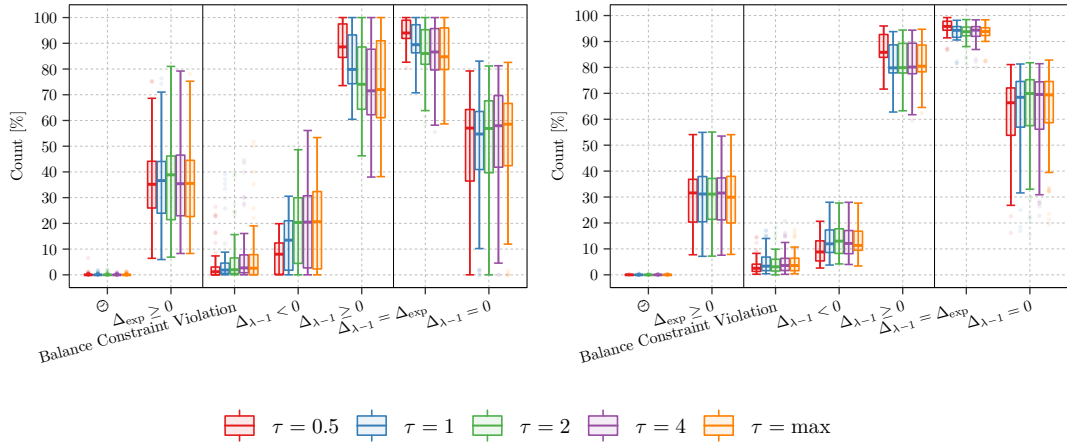


■ **Figure 11** Performance profiles comparing the solution quality for different values of τ that controls the available parallelism in our scheduler which is initialized with $\min(\min(t, \frac{k(k-1)}{2}), \tau \cdot k)$ threads.

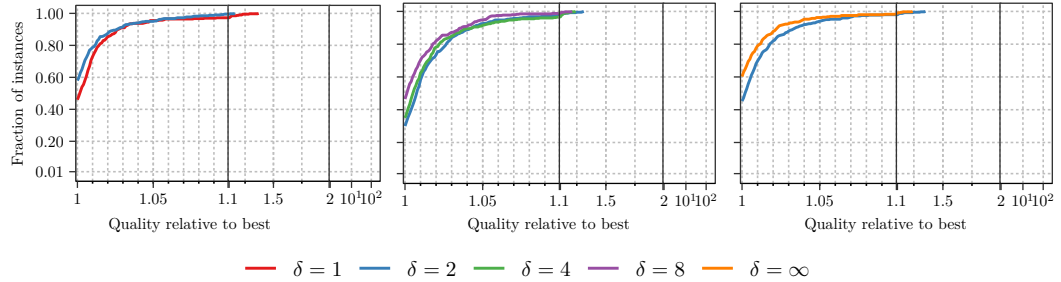
Scheduler Parallelism. The scheduler starts $\min(\min(t, \frac{k(k-1)}{2}), \tau \cdot k)$ threads which process the block pairs of the quotient graph in parallel. We evaluated Mt-KaHyPar-D-F with

$\tau \in \{0.5, 1, 2, 4, \infty\}$, $k \in \{2, 8, 16, 64\}$, $\varepsilon = 0.03$ and 3 repetitions on a subset of set B^4 and machine B. All configurations use 64 threads.

Figure 11 shows that all evaluated configurations for τ produces partitions with comparable solution quality. Mt-KaHyPar-D-F with $\tau = 1$ is faster than all other configurations. Figure 12 shows the number of interferences between the threads for increasing values of τ in percentage. We can see that the number of conflicts significantly increases for $\tau \geq 1$. This also explains that the running times slightly increase for $\tau > 1$. Applying the move sequences fails more often for larger values of τ , which slows down the convergence of the scheduling algorithm. Therefore, we choose $\tau = 1$.



■ **Figure 12** Conflict rates for different values of τ with $k \in \{8, 16\}$ (left) and $k = 64$ (right) on a subset of set B. The ticks are explained in Figure 9.



■ **Figure 13** Performance profiles comparing the solution quality if we restrict the distance of each node to the cut hyperedges to be smaller or equal to δ when we grow the region B .

Maximum BFS Distance. If we grow the region B (defines the flow network) around the cut hyperedges of a bipartition, we restrict the distance of each node to the cut hyperedges to be smaller than or equal to δ . We evaluate Mt-KaHyPar-D-F with $\delta \in \{1, 2, 4, 8, \infty\}$, $k \in \{2, 8, 16, 64\}$, $\varepsilon = 0.03$ and 3 repetitions on a subset of set A^5 and machine B. All configurations use 16 threads.

⁴ 19 out of 94 instances: 5 VLSI, 5 SPM and 9 SAT instances.

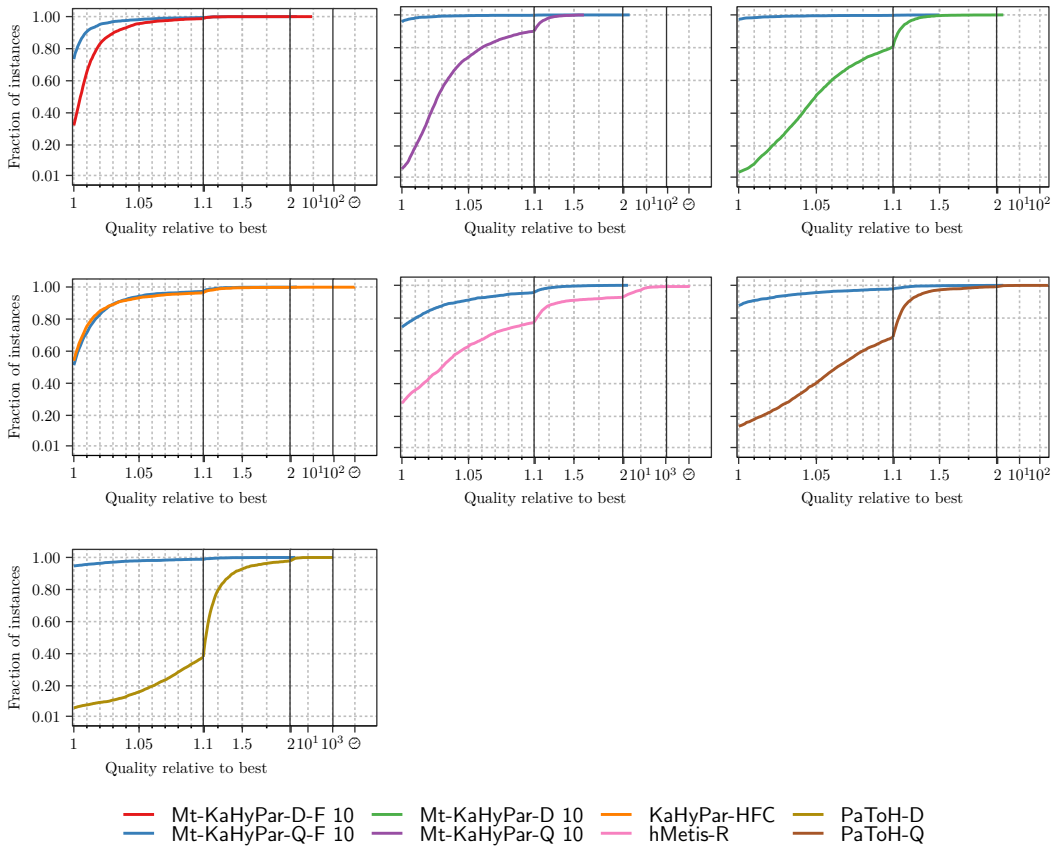
⁵ subset includes 100 instances which are also used in the parameter tuning experiments of KaHyPar [55].

Figure 13 shows that the solution quality of Mt-KaHyPar-D-F with $\delta = 2$ is slightly better compared to those with $\delta = 1$. All configurations of Mt-KaHyPar-D-F with $\delta > 2$ produces partitions that are marginally better than those with $\delta = 2$. However, Mt-KaHyPar-D-F is 17.85% slower with $\delta = 4$ than with $\delta = 2$. Therefore, we choose $\delta = 2$.

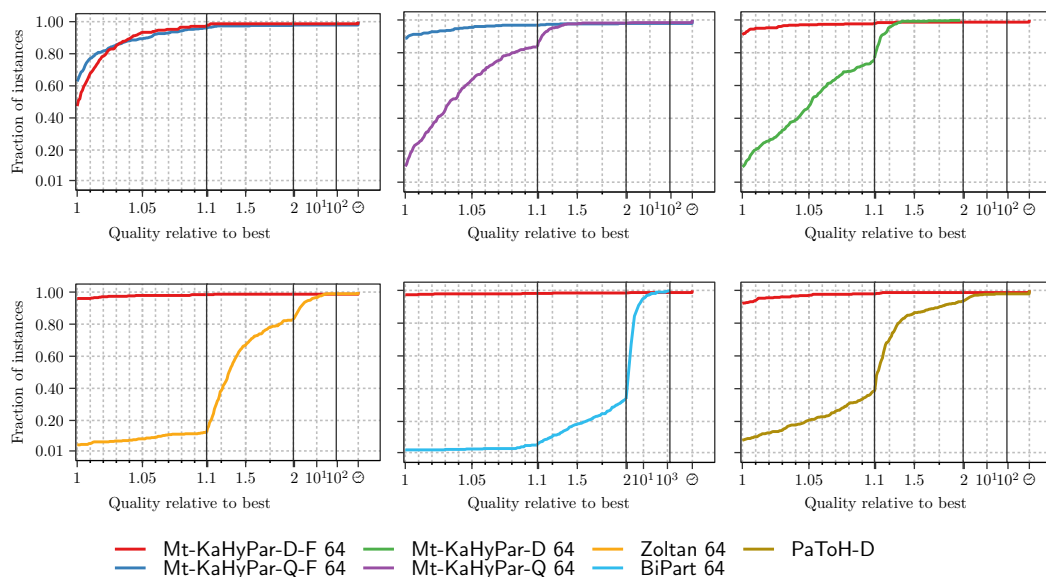
■ **Table 1** Summarizes geometric mean running times of all configurations evaluated in our parameter tuning experiments.

	$t[s]$		$t[s]$		$t[s]$
$\delta = 1$	0.99	$\tau = 0.5$	14.63	Mt-KaHyPar-D-F -BP	2.96
$\delta = 2$	1.24	$\tau = 1$	12.35	Mt-KaHyPar-D-F +BP	2.73
$\delta = 4$	1.46	$\tau = 2$	12.87	Mt-KaHyPar-Q-F -BP	5.25
$\delta = 8$	1.6	$\tau = 4$	13.34	Mt-KaHyPar-Q-F +BP	5.08
$\delta = \infty$	1.65	$\tau = \max$	13.01		

B Pairwise Comparisons with other Algorithms

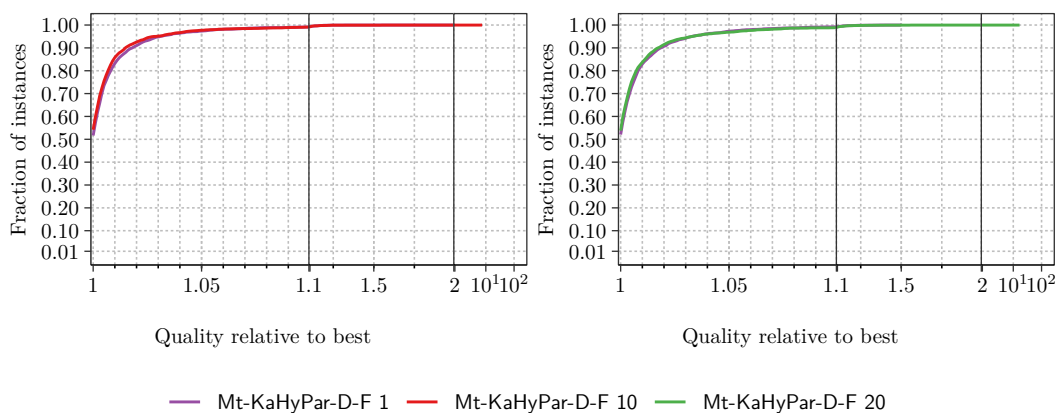


■ **Figure 14** Performance profiles comparing solution quality of Mt-KaHyPar-Q-F with different partitioners individually on set A.

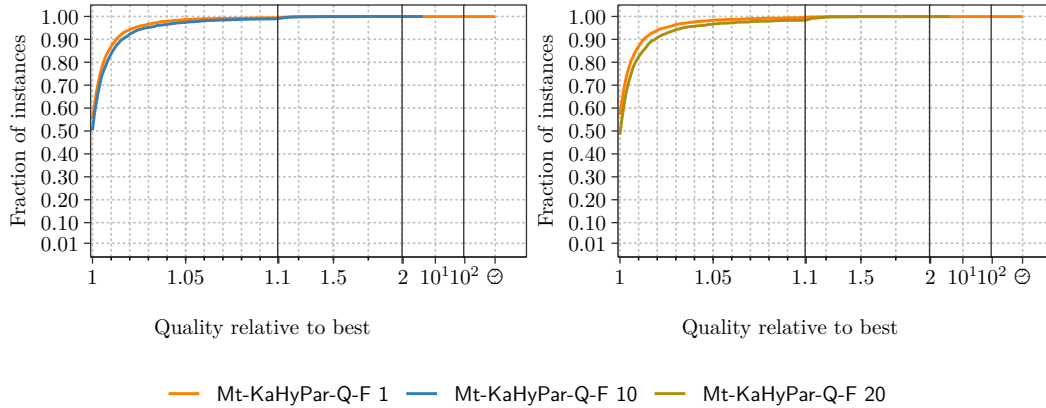


■ **Figure 15** Performance profiles comparing solution quality of Mt-KaHyPar-Q-F with different partitioners individually on set B.

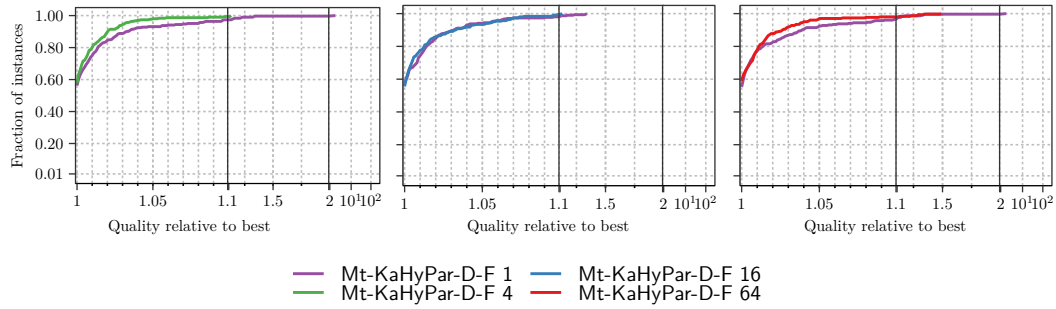
C Quality with Increasing Number of Threads



■ **Figure 16** Performance profiles comparing solution quality of Mt-KaHyPar-D-F with increasing number of threads on set A.



■ **Figure 17** Performance profiles comparing solution quality of Mt-KaHyPar-Q-F with increasing number of threads on set A.



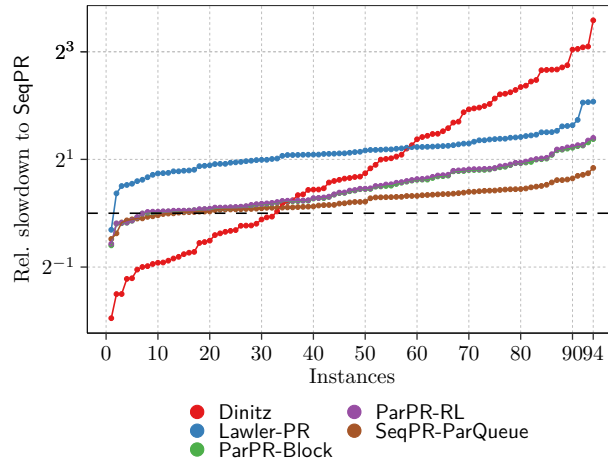
■ **Figure 18** Performance profiles comparing solution quality of Mt-KaHyPar-D-F with increasing number of threads on set B.

■ **Table 2** Summarizes geometric mean running times of Mt-KaHyPar with increasing number of threads on set A and B.

Algorithm	Set A		Set B		
	$t[s]$	Algorithm	$t[s]$	Algorithm	
Mt-KaHyPar-Q-F 1	34.3	Mt-KaHyPar-D-F 1	15.15	Mt-KaHyPar-D-F 1	163.96
Mt-KaHyPar-Q-F 10	5.08	Mt-KaHyPar-D-F 10	2.73	Mt-KaHyPar-D-F 4	52.88
Mt-KaHyPar-Q-F 20	3.78	Mt-KaHyPar-D-F 20	2.24	Mt-KaHyPar-D-F 16	22.17
				Mt-KaHyPar-D-F 64	15.44

D Flow Algorithms

In Figure 19 we plot the running time of different flow algorithms relative to a sequential hypergraph-based FIFO push-relabel implementation (SeqPR). The instances used are the networks that we extracted for the scalability experiments. We measure the time for computing a maximum preflow. In case of Dinitz algorithm the measurement also includes the time for deriving the source-side cut. The parallel algorithms are run with one thread, in order to investigate the overheads of using parallel data structures and loop constructs. As we can see, the graph-based push-relabel implementation (LawlerPR) is consistently a factor of two or more slower. Note that all push-relabel versions use the additional capacities



■ **Figure 19** Single-threaded running times of the evaluated flow algorithms relative to a sequential push-relabel implementation (SeqPR).

optimization from Section 8.3. Using parallel queues for active nodes and global relabeling in the sequential FIFO code (SeqPR-ParQueue) is consistently slower, but not by much. In previous versions of the framework [26, 27], Dinitz algorithm [20] was used because it is well suited for the incremental flow problems of FlowCutter. This may have been an oversight, as Dinitz performs worse than SeqPR on roughly $\frac{2}{3}$ of the instances, often by a substantial margin; though this measurement does not consider incremental flow problems. As opposed to the push-relabel versions, SeqPR does not strictly outperform Dinitz, since Dinitz is noticeably faster on $\frac{1}{3}$ of the instances. We consider two parallel push-relabel implementations that differ in the way they address the relabeling bug (confer Section 8.2): run global relabeling before termination (ParPR-RL) or block nodes from relabeling after being pushed to (ParPR-Block). They perform completely equivalently. We observe very moderate slowdowns over SeqPR, ranging mostly between 1 and 2.